

**Enzymatic conversion of carbon dioxide**

Journal:	<i>Chemical Society Reviews</i>
Manuscript ID:	CS-TRV-02-2015-000182.R1
Article Type:	Tutorial Review
Date Submitted by the Author:	12-May-2015
Complete List of Authors:	Shi, Jiafu; Tianjin University, School of Environment Science and Engineering Jiang, Yanjun; Hebei University of Technology, School of Chemical Engineering and Technology Jiang, Zhongyi; Tianjin University, School of Chemical Engineering and Technology Wang, Xueyan; Tianjin University, School of Chemical Engineering and Technology Wang, Xiaoli; Tianjin University, School of Chemical Engineering and Technology Zhang, Shaohua; Tianjin University, School of Chemical Engineering and Technology Han, Pingping; Tianjin University, School of Chemical Engineering and Technology Yang, Chen; Tianjin University, School of Chemical Engineering and Technology

A list of the key learning points

1. Major routes of enzymatic conversion of CO₂ in cells
2. Reaction processes/mechanisms of CO₂ conversion catalyzed by single enzyme (*oxidoreductases or lyases*)
3. Reaction processes/mechanisms of CO₂ conversion catalyzed by multiple enzymes
4. Strategies for designing and constructing enzyme catalysis systems with high activity and stability
5. Future outlook and perspectives on enzymatic conversion of CO₂

Enzymatic conversion of carbon dioxide

*Jiafu Shi^{1, 2, 3, †}, Yanjun Jiang^{4, †}, Zhongyi Jiang^{1, 3, *}, Xueyan Wang^{1, 3}, Xiaoli Wang^{1, 3}, Shaohua Zhang^{1, 3},
Pingping Han^{1, 3}, Chen Yang^{1, 3}*

¹ *Key Laboratory for Green Chemical Technology of Ministry of Education, School of Chemical Engineering and Technology, Tianjin University, Tianjin 300072, China*

² *School of Environmental Science and Engineering, Tianjin University, Tianjin 300072, China*

³ *Collaborative Innovation Center of Chemical Science and Engineering (Tianjin), Tianjin, 300072, China*

⁴ *School of Chemical Engineering and Technology, HeBei University of Technology, Tianjin 300130, China*

[†] *JF Shi and YJ Jiang contributed equally.*

Abstract:

With the continuous increase of fossil fuels consumption and the rapid growth of atmospheric CO₂ concentration, the harmonious state between human and nature faces severe challenges. Exploring green and sustainable energy resources and devising efficient methods for CO₂ capture, sequestration & utilization are urgently required. Converting CO₂ into fuels/chemicals/materials, as an indispensable element for CO₂ capture, sequestration & utilization, may offer a win-win strategy to both decrease the CO₂ concentration and achieve the efficient exploitation of carbon resource. Among the current major methods (including chemical, photochemical, electrochemical and enzymatic methods), the enzymatic method, which is inspired by the CO₂ metabolic process in cells, offers a green and potent alternative for efficient CO₂ conversion due to its superior stereo-specificity and region/chemo-selectivity. Thus, in this *tutorial review*, we will firstly provide a brief background about the enzymatic conversion for CO₂ capture, sequestration & utilization. Next, six major routes of the CO₂ metabolic process in cells, which are taken as the inspiration source for the construction of enzymatic systems *in vitro*, will be depicted. Then, the description will focus on the state-of-the-art routes for the catalytic conversion of CO₂ by single enzyme and multienzyme. Some emerging approaches and materials utilized for constructing single-enzyme/multienzyme systems to enhance the catalytic activity/stability will be highlighted. Finally, a summary about the current advances and the future perspectives of the enzymatic conversion of CO₂ will be presented.

1. Introduction

Carbon capture, sequestration & utilization (CCSU) have been widely recognized as an efficient option for reducing the atmospheric CO₂ concentration. Generally, CO₂ capture can be regarded as the process of capturing waste CO₂ from specific sources, such as fossil fuel power plants; CO₂ sequestration can be regarded as the process of transporting/depositing enriched CO₂ to a storage site (mineralization or landfill); and CO₂ utilization can be regarded as the process of directly using CO₂ as a reaction medium or transforming renewable CO₂ into useful chemicals, materials or fuels. For each process, some relatively mature technologies at industrial scale have been developed, such as alkaline absorption process (for CO₂ capture), mineralization process, landfill process (for CO₂ sequestration), supercritical CO₂ extraction process, urea synthesis process, methanol synthesis process, carboxylation of phenols, carboxylation of epoxides and carboxylation of pyrrole (for CO₂ utilization). Numerous bench-scale or industrial-scale technologies have also been developed for enhancing the efficiency of CO₂ capture, sequestration & utilization. For most of the existing technologies

except some physical processes (landfill process and supercritical CO₂ extraction process), the CO₂ fixation/conversion reaction is undoubtedly a key and common step.¹⁻⁶ So far, four major methods, including chemical, photochemical, electrochemical and enzymatic methods, have been exploited for catalyzing the CO₂ fixation/conversion reaction. For the first three methods, the selectivity is often low due to the abundant/stable form of carbon element in the molecule of CO₂ and the difficulty in acquiring high-performance catalysts. The enzymatic method may provide an eco-friendly and promising way for efficient CO₂ fixation/conversion because of its superior stereo-specificity and region/chemo-selectivity. Additionally, in the past decade, several excellent review papers about the catalytic conversion of CO₂ have been published, most of which focus on converting CO₂ through chemical or chemical-based methods.¹⁻⁶ Only one review paper offers an overview on biosynthetic routes (*in vivo*) for CO₂-fixation and a summary of detoxification processes (*in vitro*) catalyzed by lyases.¹ To the best of our knowledge, there is no review paper fully concerning the enzymatic conversion of CO₂ *in vitro*. Thus, in the following parts of this *tutorial review*, we will firstly give a summary of the CO₂ metabolic process in cells, especially the CO₂ fixation/conversion reactions. The state-of-the-art reaction routes and mechanisms for the catalytic conversion of CO₂ by single enzyme and multienzyme (*in vitro*) will be subsequently depicted with sporadic remarks. Some emerging approaches and materials utilized for constructing single-enzyme/multienzyme systems to enhance the catalytic activity and stability will be briefly described. Finally, the bottleneck problems of enzymatic conversion of CO₂ as well as the future perspectives will be presented.

2. Enzymatic conversion of CO₂ in cells

In nature, the fixation/conversion of CO₂ into organic material is a prerequisite for life and sets the starting point of biological evolution. In order to make the biological evolution proceed efficiently, cells adopt six major routes (including Calvin cycle, reductive citric acid cycle, reductive acetyl-CoA route, 3-hydroxypropionate cycle, 3-hydroxypropionate/4-hydroxybutyrate cycle and dicarboxylate/4-hydroxybutyrate cycle) for presenting the CO₂ metabolic process. In this section, these six major routes of the CO₂ metabolic process in cells will be illustrated (**Figure 1** and **Table S1**, specific information can also be found in **Figure S1-S6**),^{7,8} which offers promising reaction routes for the conversion of CO₂ and the construction of enzymatic systems *in vitro*.

Substrate/product in blue colour is the one where we start to describe the cycle/route in the following parts. Standard free energy changes (ΔG° kJ/mol, calculated from the standard free energies of formation at 25 °C) for the CO₂ fixation/conversion steps are also added in the following description of the six cycles/routes.^{7,8}

The Calvin cycle is one of the most important biosynthetic cycles on earth, which is used by majority of photosynthetic organisms (such as plants, algae, cyanobacteria, most aerobic or facultative aerobic *Eubacteria*) to incorporate CO₂ into cell carbon cycle (**Figure 1a**). Thus, this cycle is, by far, the dominant method for CO₂ conversion in nature. In general, there are three stages and three key enzymes involved in Calvin cycle. The three stages encompass CO₂ fixation (carboxylation, $\Delta G^{\circ} < 0$ kJ/mol, specific data is unavailable), CO₂ reduction and regeneration of CO₂ receptor. In the first stage, 1,5-bisphosphate ribulose bisphosphate carboxylase (Rubisco) catalyzes the reaction between CO₂ and 1,5-bisphosphate ribulose to form 3-phosphoglycerate (3 carbon compounds). Next, 3-phosphoglycerate accepts a Pi from ATP to yield 1,3-diphosphoglycerate, and further reduced to 3-phosphate glyceraldehyde by phosphoglyceraldehyde dehydrogenase. In the final stage, five-sixths amount of the acquired 3-phosphate glyceraldehyde transforms to 5-phosphate ribulose through a series of enzymatic reactions. Next, phosphoribulokinase activates 5-phosphate ribulose in an ATP-dependent condensation to produce 1,5-bisphosphate ribulose that will be utilized as the CO₂ receptor to trigger a next cycle. Another one-sixth amount of 3-phosphate glyceraldehyde will be converted into sugar, fatty acids, amino acids and so on.

The reductive citric acid cycle (also denoted as the reverse tricarboxylic acid cycle, the reverse TCA cycle, or the reverse Krebs cycle) is basically the citric acid cycle run reversely (**Figure 1b**), which converts CO₂ and water into carbon compounds. This cycle is discovered in the anaerobic *Chlorobium limicola*, a green phototrophic sulfur bacterium, also in some thermophillic bacteria that grows on hydrogen, and certain bacteria that grows by reducing sulfate. The reductive citric acid cycle contains four carboxylation steps. Succinyl-CoA is reductively carboxylated with CO₂ by α -ketoglutarate synthase/2-oxoglutarate synthase (the first step, $\Delta G^{\circ} +19$ kJ/mol) to form α -ketoglutarate/2-oxoglutarate at the expense of two equivalents of reduced ferredoxin. Next, α -ketoglutarate/2-oxoglutarate and CO₂ are converted (the second step, $\Delta G^{\circ} +8$ kJ/mol) into isocitrate catalyzed by isocitrate dehydrogenase at the expense of NADPH. Through subsequent isomerism, isocitrate is converted into citrate, and then cleaved into oxaloacetate and acetyl-CoA by ATP citrate lyase. The latter compound is carboxylated with CO₂, which requires the key enzyme pyruvate synthase (the third step, $\Delta G^{\circ} +19$ kJ/mol). The produced pyruvate is then activated by pyruvate kinase to yield polysphoenolpyruvate (PEP),

followed by carboxylation with bicarbonate (the fourth step, ΔG° -24 kJ/mol). As a result, oxaloacetate is generated, and finally converted into succinyl-CoA by a series of enzymes.

The reductive acetyl-CoA route is mainly found in strictly acetogenic bacteria, acetogenic *Eubacteria* and methanogenic *Euryarchaeota*. This route is proposed in 1965 by Ljungdahl and Wood, thus also called the Wood-Ljungdahl route (**Figure 1c**). Unlike Calvin cycle and reductive citric acid cycle, the reductive acetyl-CoA route is a noncyclic route. Specifically, CO_2 is initially converted into formate by NADH-dependent formate dehydrogenase ($F_{\text{ate}}\text{DH}$) (ΔG° +22 kJ/mol). Then, formate is captured by tetrahydrofolate and reduced into a methyl group, yielding methyl- H_4 folate. Methyltransferase (the corrinoid iron-sulfur protein) subsequently transfers the methyl group of methyl- H_4 folate to the cobalt center of the heterodimeric corrinoid iron-sulfur protein (Co^{I}), then acquiring the methylated corrinoid protein ($\text{CH}_3\text{-Co}^{\text{III}}$). Alternatively, CO dehydrogenase (CODH) functions to reduce CO_2 into CO (ΔG° 0 kJ/mol), while the acetyl-CoA synthase accepts the methyl group from $\text{CH}_3\text{-Co}^{\text{III}}$ and converts CO, CoASH, and the methyl group into acetyl-CoA.

The 3-hydroxypropionate cycle is discovered in *Chloroflexaceae*, a facultatively aerobic, phototrophic bacterium (**Figure 1d**). In this cycle, two molecules of bicarbonate can be fixed. One molecule of bicarbonate is bound onto acetyl-CoA by acetyl-CoA carboxylase in the presence of ATP, then yielding malonyl-CoA (ΔG° -14 kJ/mol). After sequential reduction of the terminal carboxylate group, malonyl-CoA is converted into propionyl-CoA. The propionyl-CoA is then carboxylated with the other molecule of bicarbonate to yield methylmalonyl-CoA by the activation of propionyl-CoA carboxylase (ΔG° -11 kJ/mol). Through the following isomerization rearrangement and a series of redox reactions, methylmalonyl-CoA is converted into methyl-CoA that was then split into acetyl-CoA and glyoxylate for replenishing the cycle and further utilization in cells, respectively.

The 3-hydroxypropionate/4-hydroxybutyrate cycle is a relatively novel cycle found in *Metallosphaera*. The genes for this cycle also exist in other archaea that is either microaerophiles or strict anaerobes. As shown in **Figure 1e**, this cycle can be divided into two parts with three key enzymes including acetyl-CoA carboxylase, propionyl-CoA carboxylase and pyruvate synthase. In the first part, acetyl-CoA carboxylase activates acetyl-CoA in an ATP-dependent condensation with bicarbonate, then yielding malonyl-CoA (ΔG° -14 kJ/mol). Through a five-enzyme cascade reaction, propionyl-CoA is synthesized from malonyl-CoA. Then, this propionyl-CoA is converted into methylmalonyl-CoA by propionyl-CoA carboxylase in the presence of

bicarbonate and ATP (ΔG° -11 kJ/mol). After isomerization rearrangement, methylmalonyl-CoA is quickly converted into succinyl-CoA. In the second part, succinyl-CoA is firstly reduced into 4-hydroxybutyrate. And then, one molecule of 4-hydroxybutyrate is converted into two molecules of acetyl-CoA after a series of cascade reactions with the participation of several enzymes. For these two molecules of acetyl-CoA, one assimilates CO_2 , and is converted into 3-phosphate glyceraldehyde by pyruvate synthase (ΔG° +19 kJ/mol), while the other is used to conduct a next cycle. Notably, this cycle has some similar/same intermediates in comparison to the 3-hydroxypropionate cycle, where succinyl-CoA is formed from acetate and two molecules of bicarbonate. From this point, the two routes become different.

The dicarboxylate/4-hydroxybutyrate cycle mainly functions in the anaerobic autotrophic members of *Thermoproteales* and *Desulfurococcales*, which has adapted to a facultative aerobic energy metabolism at low oxygen pressure (**Figure 1f**). This cycle starts from the reductive carboxylation of acetyl-CoA with CO_2 to generate pyruvate by pyruvate synthase (ΔG° +19 kJ/mol). The produced pyruvate is then converted into PEP, followed by carboxylation with bicarbonate to acquire oxaloacetate (ΔG° -12 kJ/mol). The subsequent reduction of oxaloacetate involves an incomplete reductive citric acid cycle that terminates at succinyl-CoA. The generated succinyl-CoA is further reduced into succinic semialdehyde and then into 4-hydroxybutyrate. Afterwards, one molecule of 4-hydroxybutyrate is converted into two molecules of acetyl-CoA *via* normal β -oxidation reactions. For the two molecules of acetyl-CoA, one is used for subsequent biosynthesis and the other serves as a CO_2 receptor for the next cycle.

As observed in the above-mentioned six major routes, the carbon source is either CO_2 or bicarbonate, which primarily depends on the "enzyme" in a specific CO_2 fixation/conversion reaction. Just owing to the difference in the carbon source, the fast and effective (inter)conversion between CO_2 and bicarbonate is highly required. In this regard, nature have evolved an efficient enzyme, carbonic anhydrase (CA), which can catalyze the (inter)conversion between CO_2 and bicarbonate in a fast and controllable manner in cells. As this enzyme and the (inter)conversion reaction is ubiquitous in cells (microorganisms, plants, animals, *etc.*), corresponding information is not presented in **Figure 1**.

Collectively, for all the six major routes of the CO_2 metabolic process in cells, the CO_2 fixation/conversion reaction is particularly important, in which oxidoreductases, synthases and lyases play crucial roles in accelerating the reaction rate and altering the reaction direction. To maintain the stability of such a complicated metabolic process, cells also create appropriate physicochemical microenvironments to suppress the

denaturation of enzymes. Inspired by this, the conversion of CO₂ *in vitro* catalyzed by the enzyme extracted/screened from cells may provide a high-efficiency way to accomplish the CO₂ capture, sequestration & utilization.

3. Conversion of CO₂ by single enzyme *in vitro*

Directly adopting the single enzyme (oxidoreductases, synthases or lyases) that is in charge of accomplishing the CO₂ fixation/conversion reaction in cells to catalyze the conversion of CO₂ *in vitro* seems a feasible way for CO₂ capture, sequestration and utilization. However, the reactions conducted by synthases (acetyl-CoA synthase, pyruvate synthase, acetyl-CoA carboxylase, *etc.*) usually involve CoA-containing substrates, and the acquired products are uncommon and often useless in our daily life, which make the synthases unsuitable for *in vitro* applications. Therefore, directly inspired from the six major routes, only other two classes of enzymes, oxidoreductases (F_{ate}DH, CO₂ reductase, CODH, remodeled nitrogenase, *etc.*) and lyases (CA), have been discovered/extracted from specific organisms. Correspondingly, several kinds of fuels/chemicals/materials, including formate, CO, methane, bicarbonate, *etc.*, have been successfully synthesized. This section will describe the state-of-the-art reaction routes for the catalytic conversion of CO₂ by single enzyme. In addition, enlightened by the existing form and physicochemical environment of enzymes in cells, some advanced approaches and materials utilized for constructing enzymatic systems with enhanced catalytic activity and stability will also be described.

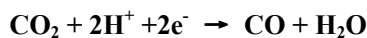
3.1 Conversion of CO₂ by oxidoreductases

Theoretically, an oxidoreductase is a kind of enzyme that catalyzes the transferring of electrons from one molecule (the reductant or electron donor) to another (the oxidant or electron acceptor). During the redox reaction, NADPH/NADP⁺ or NADH/NAD⁺ is employed as essential cofactor(s). The aim of converting CO₂ by an oxidoreductase is to reduce the oxidation state of carbon element, and acquire carbon-based energy resources.

3.1.1 Conversion of CO₂ to formate by formate dehydrogenase (F_{ate}DH) or carbon dioxide (CO₂) reductase

The first choice of products from the conversion of CO₂ catalyzed by oxidoreductases should be formate or CO (**Equation 1** and **2**). Undoubtedly, CO is a kind of important chemicals and fuels. Alternatively, formate is also an important chemical as it can be utilized for methanol production, hydrogen production, direct formic acid fuel cells, *etc.*





2)

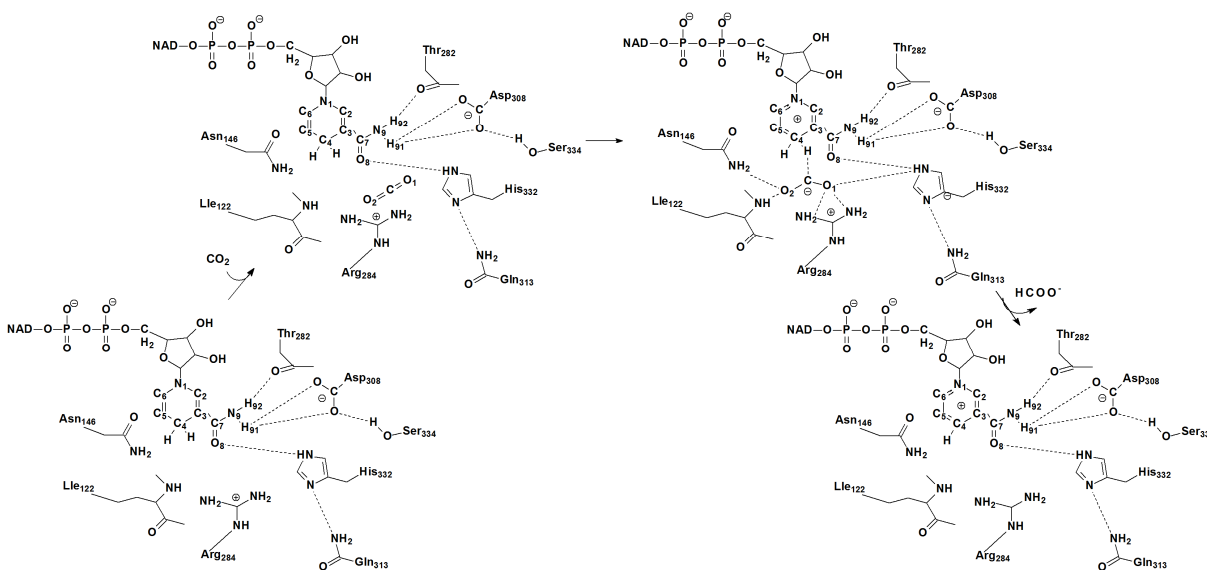


Figure 2. The mechanism for the reduction of CO_2 to formate by NADH-dependent $\text{F}_{\text{ate}}\text{DH}$.⁹

As mentioned in the third route of the CO_2 metabolic process (Reductive acetyl-CoA route), CO_2 could be fixed and converted into formate *in vivo* catalyzed by $\text{F}_{\text{ate}}\text{DH}$ (a typical oxidoreductase) with NADH as a cofactor. The mechanism for the reduction of CO_2 to formate by this NADH-dependent $\text{F}_{\text{ate}}\text{DH}$ can be simply proposed as the direct transferring of hydride from the C_4 atom of the pyridine ring in NADH to the C atom of CO_2 (**Figure 2**). CO_2 and NADH are positioned in close proximity to facilitate hydride transferring. After the generation of formate, NAD^+ with a bipolar conformation is left.⁹ Intrigued by this route, several research groups (such as Baeg's group, Amao's group, Müller's group, Hirst's group, Jiang's group, *et al.*)¹⁰⁻¹⁶ have utilized NADH-dependent $\text{F}_{\text{ate}}\text{DH}$ to convert CO_2 and systematically investigated the catalytic performance. In order to acquire high stability (especially recycling stability) of the enzymes, Jiang and co-workers¹⁵ encapsulated NADH-dependent $\text{F}_{\text{ate}}\text{DH}$ from *Candida boidinii* into a series of millimetre-sized sol-gel carriers, including silica gels, alginate-silica gels, hydroxyapatite-polysaccharide gels, *etc.* Once applied for reducing CO_2 at the expense of NADH, the immobilized enzymes exhibited desirable activity and high stability (formate yield could reach high up to *ca.* 95.6% for 8-h reaction) primarily because the suitable structures of the carriers offered favourable microenvironments to preserve the 3-D structure of the enzymes. Unfortunately, in the above case, the cofactor in either free or immobilized systems was a sacrificial reagent. Considering its high cost, coupling of the enzymatic conversion of CO_2 and the cofactor regeneration was urgently required.

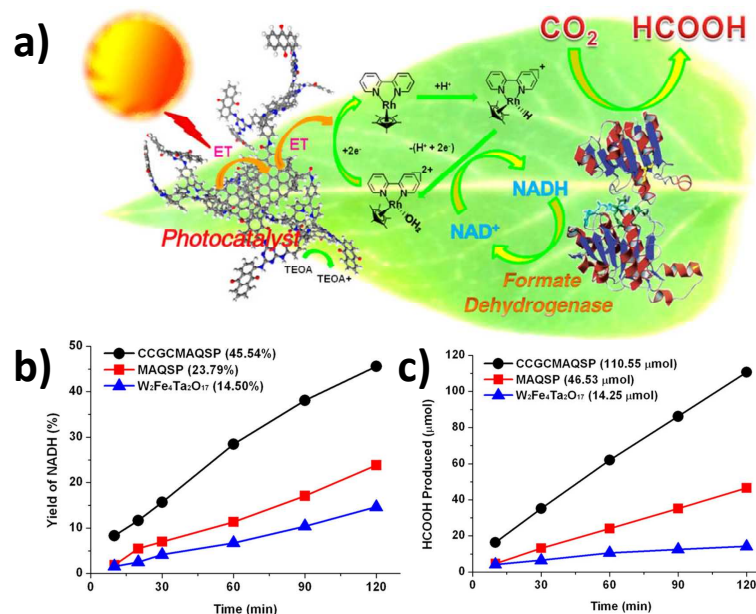


Figure 3. a) Artificial photosynthesis of formate from CO₂ catalyzed by the photocatalyst-enzyme coupled system under visible light; and b) time dependence of NADH yield and c) formate production using the photocatalyst-enzyme coupled system under visible light irradiation. Reproduced with permission from ref. 12. Copyright 2012 American Chemistry Society.

To achieve this goal, an artificial photosynthesis system through coupling the graphene-based photocatalyst and NADH-dependent F_{ate}DH was established by Baeg and co-workers¹². The photosynthesis system (CCGCMAQSP) mainly composed of the chemically converted graphene (CCG), the chromophore covalently bound with CCG (multianthraquinone substituted porphyrin, MAQSP), and a kind of enzyme (NADH-dependent F_{ate}DH) in free form. The mechanism of this photosynthetic process was illustrated in **Figure 3**. Specifically, the absorption of photon firstly occurred as a transition between localized orbitals around the chromophore (MAQSP). The generated electrons transferred and reached the rhodium complex *via* the graphene surface. After accepting the electrons, the rhodium complex was reduced. The reduced rhodium complex extracted a proton from the bulk aqueous solution, transferred the electrons and a hydride to NAD⁺ for NADH regeneration. Then, the regenerated NADH was consumed during the CO₂-to-formate conversion process, and finally the whole regeneration cycle was accomplished. Baeg and co-workers¹² also constructed other two kinds of artificial photosynthesis systems through coupling W₂Fe₄Ta₂O₁₇ and MAQSP photocatalysts with NADH-dependent F_{ate}DH. In **Figure 3b** and **3c**, the investigations of NADH regeneration and formate production clearly revealed the superiority of the CCGCMAQSP-based artificial photosynthesis system over

the other two systems. Based on the previous exploitations, Amao and co-workers¹¹ also constructed an immobilized artificial leaf device through co-immobilizing chlorin-e6 (as a photosensitised dye), a viologen with a long alkyl chain (as an electron donor) and NAD(P)H-dependent $F_{\text{atc}}\text{DH}$ from *Saccharomyces cerevisiae* on a silica gel-based substrate for catalytically converting CO_2 . When the CO_2 -saturated NAD(P)H aqueous solution (the cofactor) was flowed onto the artificial leaf device under visible light irradiation, the formate concentration increased with the prolongation of irradiation time, indicating the essential role of solar energy on the production of formate from CO_2 . More importantly, this artificial leaf device could enhance the enzyme stability and regenerate the cofactor simultaneously.

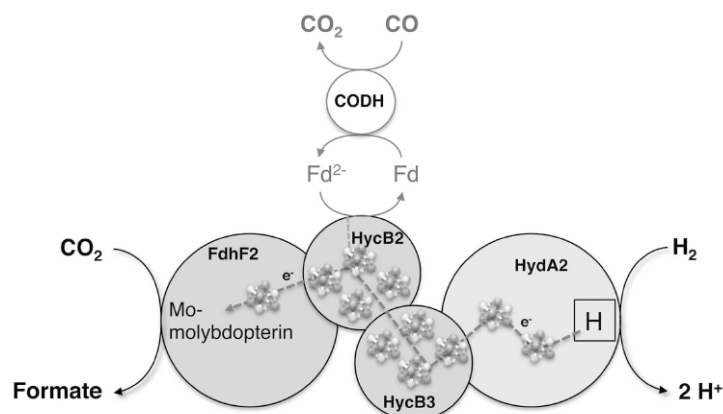


Figure 4. The model of the hydrogen-dependent CO_2 reductase (HDCR) from *Acetobacterium woodii*. Electrons for CO_2 reduction are either provided by the hydrogenase subunit iron-iron hydrogenase (HydA2), where hydrogen oxidation takes place, or by the reduced ferredoxin. The latter can be reduced by using CO and CO dehydrogenase (CODH). Electrons are delivered to the active site for CO_2 reduction in selenium-containing formate dehydrogenase (FdhF2) via the electron-transferring subunits (HycB2/3). Iron sulfur clusters are shown in the central part of this figure.^{10, 14}

Previous studies indicated that the ion-type cofactor, mainly referring to NADH, was required in the catalytic reduction of CO_2 to formate when adopting NADH-dependent $F_{\text{atc}}\text{DH}$ as the catalyst. The high cost and difficult availability of an ion-type cofactor may restrict the further applications of this enzymatic route. Very recently, a great breakthrough was reported by Müller and co-workers.^{10, 14} They discovered a bacterial hydrogen-dependent CO_2 reductase (HDCR, from the acetogenic bacterium *Acetobacterium woodii*) that could directly use H_2 as a "cofactor" for converting CO_2 into formate. The HDCR enzyme was composed of four different subunits (**Figure 4**), including a putative formate dehydrogenase (FdhF1/2) and an iron-iron

hydrogenase (HydA2) as the two large subunits neighbored by two small electron transfer subunits (HycB2/3). Amongst, the FdhF1/2 acted as the catalyst for reducing CO_2 into formate; HydA2 was in charge of activating/oxidizing H_2 into two H^+ accompanied with acquiring two electrons; and HycB2/3 was responsible for transferring the two electrons from HydA2 to FdhF1/2. Once utilized for the catalytic conversion of CO_2 and H_2 to formate, the reaction rate was high up to $10 \text{ mmol min}^{-1} \text{ mg}^{-1}$. The TOF was calculated to be $101,600 \text{ h}^{-1}$ that was nearly 1500 times higher than that of chemical catalysis ($\sim 70 \text{ h}^{-1}$). One remarkable advantage of this route should be the independence of the external ion-type cofactor. Moreover, as illustrated in **Figure 4**, the HDCR can also catalyze the reduction of CO_2 with reduced ferredoxin as a "cofactor". As ferredoxin can be reduced by CO dehydrogenase (CODH) from *Acetobacterium woodii*, formate can also be produced from CO once integrating the HDCR, CODH and ferredoxin into one system. Considering that industrially produced H_2 often contained certain amount of CO, this integrated system may allow the complete conversion of gas mixtures (or syngas) containing H_2 , CO_2 , and CO.

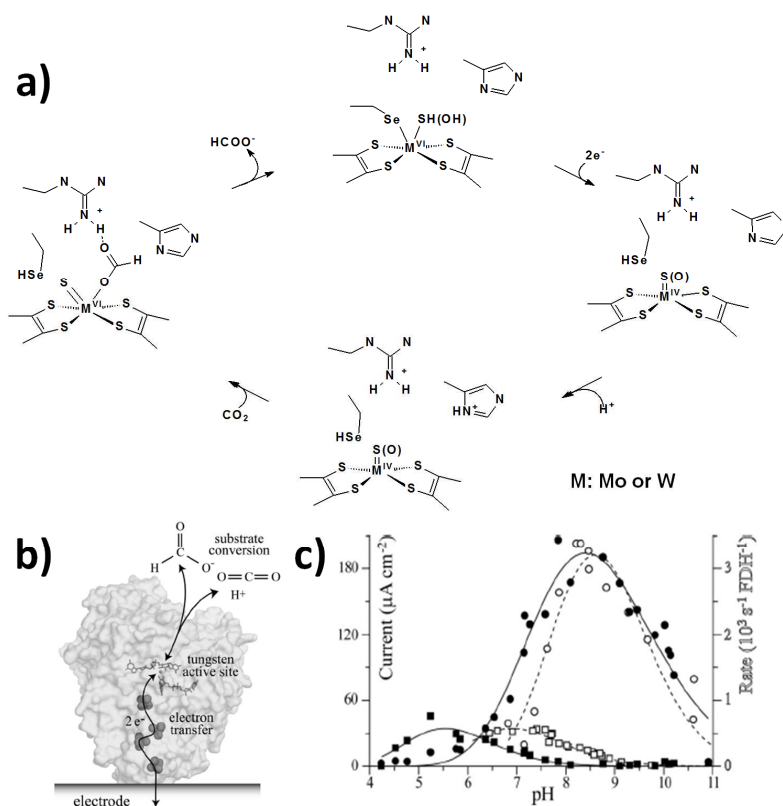


Figure 5. a) The proposed mechanism for the reduction of CO_2 to formate by molybdenum- or tungsten-containing $\text{F}_{\text{ate}}\text{DH}$,^{6, 17} b) the schematic representation of the catalytic (inter)conversion between CO_2 and formate by $\text{F}_{\text{ate}}\text{DH}$ adsorbed on an electrode surface (herein, the structure shown in **Figure 5a** is that of the tungsten-containing $\text{F}_{\text{ate}}\text{DH}$ from *Desulfovibrio gigas*); c) the kinetics of this catalytic reaction by

tungsten-containing $F_{\text{ate}}\text{DH}$ as a function of pH value. Current densities from the first voltammetric scan in 10 mM formate and 10 mM CO_2 at 0.25 V overpotential are compared to data from conventional assays in solution in 10 mM formate or 10 mM CO_2 . (*Open square, rate of CO_2 reduction in solution; filled square, rate of catalytic reduction of CO_2 ; open circle, rate of formate oxidation in solution; filled circle, rate of catalytic oxidation of formate.*) Reproduced with permission from ref. 13. Copyright 2012 National Academy of Sciences, United States.

Another breakthrough to address the issue of cofactor consumption/regeneration should be the finding of the NADH-independent $F_{\text{ate}}\text{DH}$, of which the active site is molybdenum or tungsten center.^{6, 13, 17} As a proposed mechanism for the reduction of CO_2 by this kind of $F_{\text{ate}}\text{DH}$, two electrons are firstly transferred to the molybdenum or tungsten center, and then the Mo^{VI} or W^{VI} ion is reduced into the Mo^{IV} or W^{IV} ion. The reduced active site features a square pyramidal molybdenum or tungsten center that is coordinated to four sulfur atoms from two pyranopterin ligands in the basal plane and a fifth sulfur atom in an apical position. The selenocysteine ligand is simultaneously released from the active site. Afterwards, one H^+ ion is transferred to the N atom of the imidazole ring to form an intermediate that is utilized as a proton donor in the subsequent step. Once CO_2 is contacted with the active site, a C-H bond is formed and a C=O bond is cleaved into a C-O bond. Accordingly, formate is formed. During the formation process of C-H bond, the arginine residue assists in orienting the formate ligand for the proton removal/delivery by the histidine residue. Obviously, different from the hydride transfer mechanism of the NADH-dependent $F_{\text{ate}}\text{DH}$, the molybdenum- or tungsten-containing enzymes transfer the two electrons and the H^+ /proton to different sites. Based on this finding, Hirst and co-workers utilized both molybdenum- and tungsten-containing $F_{\text{ate}}\text{DH}$ to convert CO_2 into formate.^{13, 17} Taking tungsten-containing $F_{\text{ate}}\text{DH}$ as an example, they directly adsorbed $F_{\text{ate}}\text{DH}$ from *S. fumaroxidans* on an electrode surface, which exhibited high efficiency in the catalytic reduction of CO_2 to formate. Briefly, as shown in **Figure 5a**, two electrons were transferred from the electrode to the active site (buried inside the insulating protein interior) by the iron-sulfur clusters, thus reducing CO_2 into formate through forming a C-H bond and cleaving a C=O bond. As illustrated in **Figure 5b**, the rate for this reaction was highly sensitive to pH values, which was found to increase 6-fold from pH 7.5 to 5.5. The highest current density corresponded to an average turnover frequency of 112 s^{-1} from a monolayer of tungsten-containing $F_{\text{ate}}\text{DH}$. This value was about two orders of magnitude faster than CO_2 hydrogenation by ruthenium complexes in supercritical CO_2 and 10 times faster than photosynthetic CO_2 activation during the carboxylation of 1,5-bisphosphate ribulose by Rubisco. Notably,

in Hirst's work, the oxidation of formate was also conducted by using this system (**Figure 5b**). But no corresponding discussion was given in our *tutorial review* owing to its weak relevance to our main topic.

3.1.2 Conversion of CO_2 to carbon monoxide (CO) by carbon monoxide dehydrogenase (CODH)

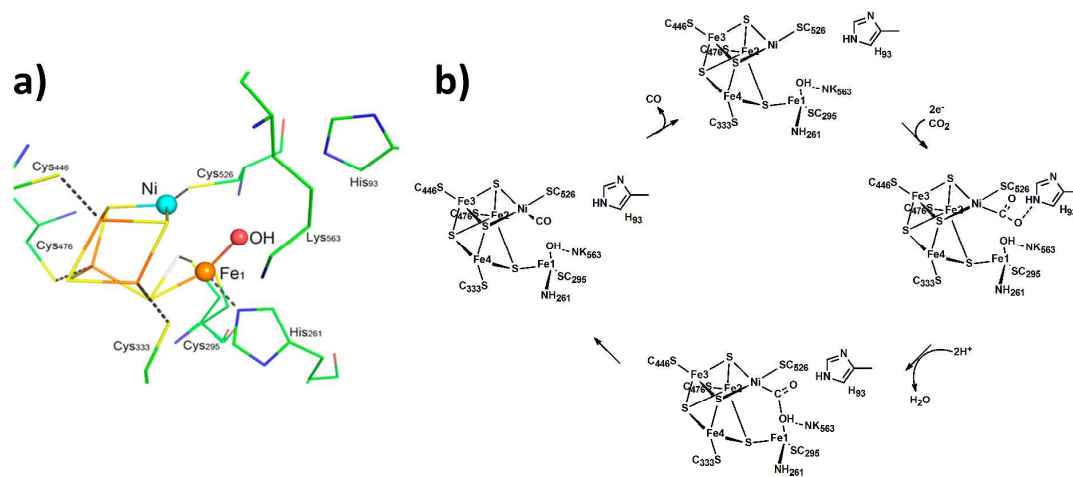


Figure 6. a) Ball-and-stick drawing of the active site of [NiFe] CODH; and b) the proposed mechanism for the reduction of CO_2 to CO by [NiFe] CODH.^{6, 18}

CO , another important product from the reduction of CO_2 , is regarded as the key feedstock for various synthetic processes, such as the Fischer-Tropsch, Monsanto and Cativa processes. Meanwhile, CO also possesses significant fuel value and can be readily converted into methanol (as a liquid fuel). In nature, the (inter)conversion between CO and CO_2 is primarily catalyzed by [NiFe] CO dehydrogenases ([NiFe] CODH). As shown in **Figure 6a**, the active site of [NiFe] CODH mainly consists of Ni and Fe centers bridged by a [3Fe-4S] cluster that positions these two metal centers in close proximity. The proposed mechanism for the reduction of CO_2 to CO by [NiFe] CODH can be illustrated in **Figure 6b**.^{6, 18} Generally, an overall two-electron process occurs during the whole reaction process: an electron transfer step to form reduced Ni center, followed by a chemical step involving CO_2 bound to the reduced Ni center, and finally a second electron transfer step. For the chemical step, CO_2 binds to the Ni atom *via* the C atom to form a Ni-C bond. Simultaneously, one of the carboxylate oxygen atoms (O_2) forms a hydrogen bond with a protonated histidine residue (H93). Loss of water from Fe1 results in the formation of a CO_2 complex, in which another oxygen atom of the CO_2 molecule, O_1 , is bound to Fe1 and forms a hydrogen bond with a protonated lysine residue (K563). Cleavage of the C- O_1 bond and loss of water result in the formation of a $\text{Ni}^{\text{II}}\text{CO}$ species. This $\text{Ni}^{\text{II}}\text{CO}$ species readily releases CO and adds water to regenerate the starting Ni^{II} complex and complete the catalytic cycle. Therefore, CO_2 binding, catalysis or even release in the enzyme appears to involve the activation by the two metal centers and additional

stabilization from appropriately positioned residues in the second coordination sphere. Inspired by this *in vivo* enzymatic reaction, researchers have devoted tremendous efforts to construct *in vitro* systems for converting CO₂ into CO efficiently.

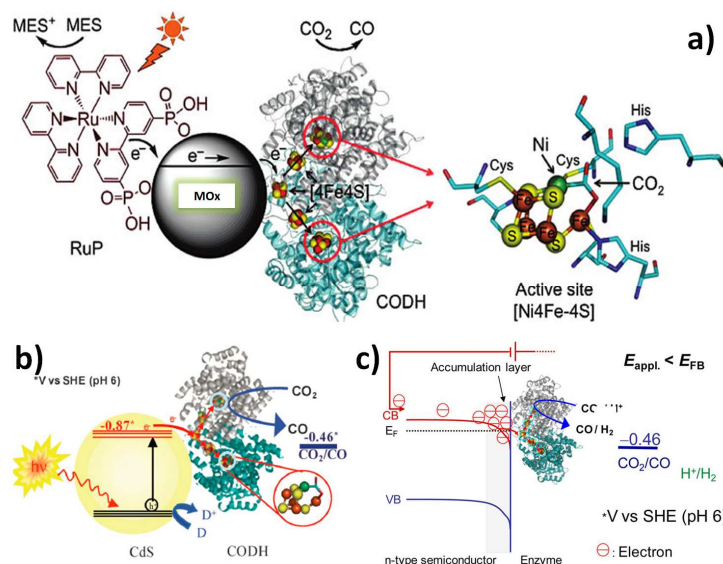


Figure 7. a) Schematic representation of CO₂ photosynthesis system upon [NiFe] CODH attached to RuP-modified *n*-type metal oxide (MOx) semiconductors. A catalytic intermediate that is the active site in the enzyme [NiFe] CODH bound with CO₂ is also shown (*right in Figure 7a*). The oxidized photosensitizer is recovered by the sacrificial electron donor. Reprinted with permission from ref. 21. Copyright 2010 American Chemistry Society; b) schematic representation of visible light-driven CO₂ reduction upon [NiFe] CODH-CdS nanocrystal assemblies in the presence of an electron donor. Reprinted with permission from ref. 23. Copyright 2012 Royal Society of Chemistry; and c) schematic representation of the formation of an electron accumulation layer at the surface of CdS or MOx when the applied electrode potential is lowered to the flatband potential (E_{FB}). The increased electron density and subsequent downward band bending facilitate efficient electron transferring to the enzyme active site *via* [Ni₄Fe₄S] clusters to reduce CO₂. Reprinted with permission from ref. 24. Copyright 2013 American Chemistry Society.

The first report of utilizing [NiFe] CODH (from *Moorella thermoacetica*) to reduce CO₂ into CO *in vitro* was implemented by Shin and co-workers.¹⁹ Since then, the most representative studies in the last decades were accomplished by Armstrong and co-workers.²⁰⁻²⁴ One of the significant advances in their investigations is the efficient combination of electrocatalysis/photocatalysis with enzymatic conversion of CO₂ to CO. Traditionally, due to the highly uphill thermodynamics of the one-electron transferring to form CO₂^{•-} ($E = -1.9$ V *vs.* SHE in

water, corrected to pH 7), the electrocatalytic/photocatalytic conversion of CO₂ usually require significant overpotentials (hundreds of mV), which will waste a lot of energy. Besides, this high-energy-input route may result in mixture of products, including CO, methane and methanol. To address this issue, Armstrong and co-workers²⁰ immobilized [NiFe] CODH on a pyrolytic graphite "edge" (PGE) electrode, and systematically evaluated the activity of this enzyme rotating at high speed in an anaerobic sealed cell. In this process, the standard reduction potential for the (inter)conversion between CO₂ and CO catalyzed by [NiFe] CODH ($E = -0.46$ V vs. SHE in water, at pH 6, or $E = -0.51$ V vs. SHE in water, corrected to pH 7) was much higher than that without a catalyst ($E = -1.9$ V vs. SHE in water, corrected to pH 7). This would then lead to a much lower required overpotential along with an extremely high selectivity for yielding a specific product (CO, ~100%). Subsequently, they incorporated photocatalysis into the enzymatic conversion of CO₂ for constructing artificial photosynthesis system.^{21, 22} Briefly, [NiFe] CODH as the catalyst and [RuII(bipy)₂(4,4'-(PO₃H₂)₂-bipy)]Br₂ (RuP; bipy=2,2'-bipyridine) as the photosensitizer were both adsorbed on a series of *n*-type MOx semiconductor nanoparticles (*e.g.*, P25 TiO₂, anatase TiO₂, rutile TiO₂, ZnO, SrTiO₃, *etc.*) to construct a photocatalyst-enzyme coupled system. The principle of CO₂ conversion process can be found in **Figure 7a**. In detail, through the excitation with visible light, RuP injected electrons into the *n*-type MOx semiconductor conduction band (*e.g.*, -0.52 V for anatase TiO₂, pH 6). These electrons were then entered [NiFe] CODH through the D-cluster, and transferred through a second [Ni₄Fe₄S] cluster to the active site, where CO₂ was reduced into CO. Through oxidation process, the photosensitive dye could be regenerated by a sacrificial electron donor (*e.g.*, (2-(N-morpholino)ethanesulfonic acid (MES), *etc.*). After carefully manipulating the factors (including coverage of enzyme and RuP on the *n*-type MOx semiconductor nanoparticles, species of semiconductors, species of electron donors, *etc.*), the photosynthesis systems prepared with P25 TiO₂ and ordinary anatase TiO₂ nanoparticles were confirmed to be the most effective catalysts with an overall turnover frequency of 0.14 s⁻¹. This system is an excellent example for the further related investigations, although the turnover frequency was relatively lower than the expected result. Obviously, [NiFe] CODH, *n*-type MOx semiconductors, RuP, and sacrificial electron donor were essential in the above system. Particularly, since most *n*-type MOx semiconductors possessed a relatively wide band gap (such as TiO₂, $E_g = 3.1$ eV), the semiconductors must be photosensitized by the co-attachment of a visible light harvesting RuP. The hole left on the RuP could be quenched by a sacrificial electron donor. To simplify and intensify this process, Armstrong and co-workers²³ developed a Ru-free system, where [NiFe] CODH was assembled on CdS nanocrystals with

visible-light harvesting capability (*the conduction band (CB) edge of bulk CdS was at $E_{CB} = -0.87$ V vs. SHE in water, at pH 6*), which could offer enough driving force to reduce CO_2 into CO (reduction potential -0.46 V vs. SHE in water, at pH 6) (**Figure 7b**). After assaying the activity of reducing CO_2 into CO under visible light through tailoring the sacrificial agents and particle size/shape (CdS nanocrystal), the average turnover frequency for the [NiFe] CODH-CdS_{nanorods} assemblies could be high up to 1.23 s⁻¹. This value was much higher than that reported by using supramolecular or semiconductor photocatalysts (<0.14 s⁻¹). Very recently, the mechanism that the light-harvesting *n*-type semiconductors altering the bias of the reversible catalysts ([NiFe] CODH) in favour of CO_2 reduction was clarified by Armstrong's and Nørskov's groups.^{24, 25} Similar conclusions were derived and summarized as follows. On the basis of the previously established models,^{24, 25} the surface electron concentration increased exponentially as the potential was lowered, and could be controlled by the difference between the flatband potential (E_{FB}) and the applied electrode potential. When the applied electrode potential was lower than E_{FB} , a transformation to metallic-like character would occur as an accumulation layer forms (**Figure 7c**). Therefore, the increase in electron density at the semiconductor-enzyme interface would favour the efficient electron transferring from the *n*-type semiconductor to the enzyme for driving the reduction process. This principle or mechanism will offer a further design criterion for the artificial chemical/energy conversion systems.

Besides the [NiFe] CODH enzyme that can directly convert CO_2 into CO, other types of oxidoreductases in nature may also render the possibility of catalyzing this reduction. Fortunately, Seefeldt and co-workers²⁶ found that nitrogenase from *Azotobacter vinelandii*, a kind of enzyme that commonly catalyzes six-electron reduction of N_2 to ammonia, could catalyze the two-electron reduction of CO_2 . To verify this possibility, CO acquired from the reduction of CO_2 was quantified by using nitrogenase as the catalyst. A time-dependent production of CO was found, providing strong evidence for the reduction of CO_2 to CO catalyzed by nitrogenase. This finding will expand the route of reducing CO_2 into CO by seeking enzymes in a much broader range.

3.1.3 Conversion of CO_2 to methane catalyzed by remodeled nitrogenase

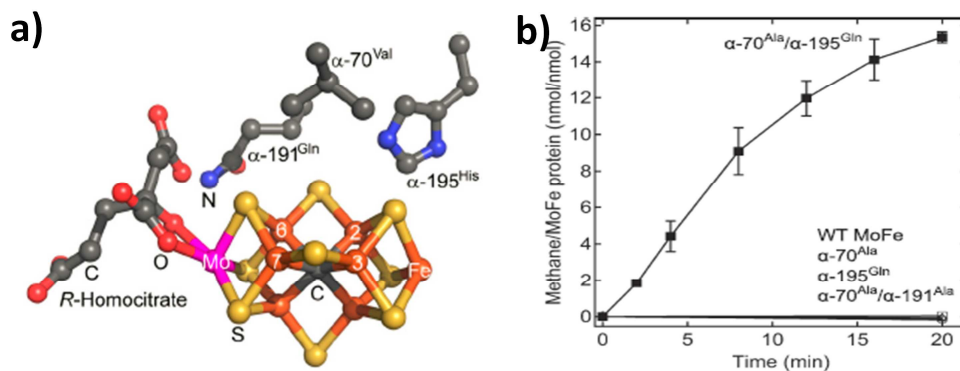


Figure 8. a) The FeMo-cofactor with some key amino acid residues (colors: Mo, magenta; Fe, rust; S, yellow; C, gray; O, red; N, blue); and b) the methane formation as a function of time for different MoFe proteins. CO₂ reduction to methane is shown as a function of time for the wild-type (or native) (○), α -70Ala (◇), α -195Gln (△), α -70Ala/ α -191Ala (□), and α -70Ala/ α -195Gln (■) MoFe proteins. Reprinted with permission from ref. 27. Copyright 2012 National Academy of Sciences.

As illustrated in the final part of the section "3.1.2 Conversion of CO₂ to carbon monoxide (CO) by carbon monoxide dehydrogenase (CODH)", nitrogenase might also be able to catalyze the two-electron reduction of CO₂ to yield CO since it can effectively catalyze the multielectron (six-electron) reduction of N₂. Fortunately, the feasibility of this reaction has been demonstrated by Seefeldt and co-workers.²⁶ At the beginning of their investigation, Seefeldt and co-workers wondered whether this nitrogenase could catalyze the eight-electron reduction of CO₂ to the level of methane. Unfortunately, when the wild-type (or native) nitrogenase was employed for reducing CO₂, no methane was detected over a 20 min-reaction (**Figure 8b**), indicating the native nitrogenase cannot trigger this reaction. Since several amino acids (α -195, α -70, α -191, *etc.*) that approached the FeMo-cofactor (the active site, **Figure 8a**) in nitrogenase played a quite important role in controlling substrate binding and reducing, substitution of these amino acids with appropriate molecules may alter the catalytic behavior. To their surprise, the remodeled nitrogenase substituting the α -195 by Gln and α -70 by Ala was able to catalyze the formation of methane from CO₂, forming up to 16 nmol (methane) nmol⁻¹ (MoFe protein) over a 20 min-reaction (**Figure 8b**). The reaction rate mainly depended on the partial pressure of CO₂ (or bicarbonate concentration) and the electron flux through the remodeled nitrogenase.



The mechanism for the reduction of CO₂ by the remodeled nitrogenase was similar to that of N₂ reduction by

the native nitrogenase (**Equation 3**).²⁷ As reported, metal-bound hydrides were an integral part of the FeMo-cofactor for activating N_2 , which was considered to participate in the initial reduction of N_2 to the intermediate diazene ($HN=NH$). Further reduction of the metal-bound diazene into two ammonia molecules was proposed after successive addition of electrons and protons. No detection of the proposed reaction intermediates (diazene $HN=NH$ or hydrazine H_2N-NH_2) suggested that the intermediates were bound to the active site until the final products were formed and released. This phenomenon could be explained by the stabilization of the key intermediates through appropriate functional groups, thus minimizing the kinetic barriers of this reaction. Similarly, the remodeled nitrogenase may also stabilize key intermediates through appropriate functional groups in the multielectron reduction of CO_2 to methane (**Equation 4**). Specifically, metal-bound hydrides may participate in the initial steps of CO_2 reduction. The possible reaction occurred in this step should be the two-electron reduction of CO_2 by hydride insertion. Further reduction of the metal-bound intermediates (*e.g.*, *metal-bound formate or metal-bound formaldehyde*) into methane could be continued once electrons and protons were successively supplied. Besides the route of CO_2 to methane, remodeled nitrogenase can also catalyze the coupling of CO_2 with acetylene, yielding predominately propylene. Collectively, the finding described in this section provides insights into the broader context of how N_2 is reduced to ammonia by enzymes. Future studies should focus on lowering the reaction barriers through stabilizing key reaction intermediates in order to reduce CO_2 into larger variety of hydrocarbons.

3.2 Conversion of CO_2 by lyases

A lyase is an enzyme that catalyzes the breaking of chemical bonds rather than hydrolysis or oxidation, and then generates a new double bond or a new ring structure. The reverse reaction (called "Michael addition") catalyzed by a lyase commonly exist in cells, which offers an enlightenment of the carboxylation of raw molecules with CO_2 to obtain valuable chemicals/materials.

3.2.1 Conversion of CO_2 to bicarbonate (or minerals) by carbonic anhydrase (CA)

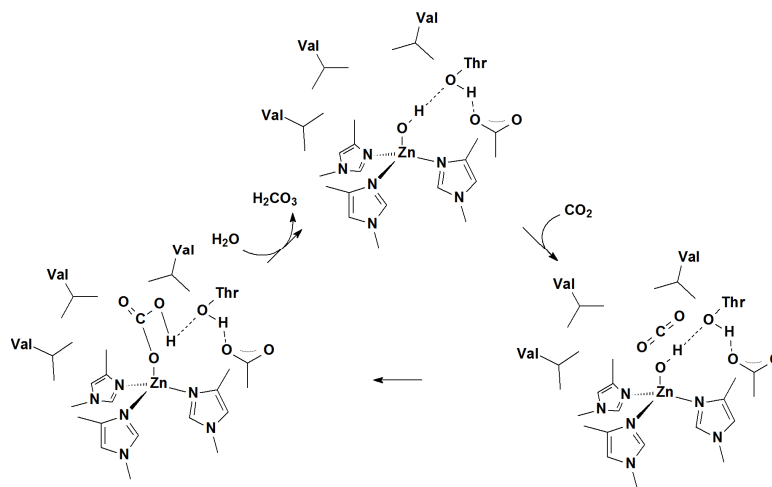


Figure 9. The proposed mechanism for the hydration of CO_2 by $[\text{Zn}] \text{CA}$.^{6, 28}



Carbonic anhydrase (CA), as a typical lyase, commonly exists in nature (mammals, plants, algae and bacteria) and mainly responsible for the (inter)conversion between CO_2 and bicarbonate to maintain the acid-base balance in blood and other tissues (**Equation 5**). CA is an archetypal example of convergent evolution, comprising at least five distinct classes of α , β , γ , δ and ζ with little structural similarity, but all the CAs compose of an active site of divalent zinc ion or related metal ion. Taking $[\text{Zn}] \text{CA}$ as an example, the proposed mechanism for the hydration of CO_2 could be described as follows (**Figure 9**):^{6, 28} the active sites of $[\text{Zn}] \text{CA}$ can be considered as a Zn^{2+} ion that is coordinated to three histidine residues and a water/hydroxide. The coordination of water increases its acidity to a pKa value of approximately 7, which allows the coordinated water to be deprotonated with weak bases to produce a hydroxide ligand. This hydroxide can then undergo a nucleophilic attack at the C atom of CO_2 to yield a bicarbonate molecule stabilized by hydrogen bonding to a Thr residue and other residues in the second coordination sphere. A hydrophobic pocket formed by three Val residues assists in the positioning of CO_2 for the nucleophilic attack by the hydroxide ligand. Displacement of bicarbonate by water could then regenerate the catalyst. Key features of this mechanism are the activation of water by binding to Zn^{2+} , the precise positioning of CO_2 in a hydrophobic pocket, and hydrogen bonding sites positioned in the second coordination sphere of Zn. Besides, the turnover frequency of $[\text{Zn}] \text{CA}$ can be high up to $\sim 10^6 \text{ s}^{-1}$, making $[\text{Zn}] \text{CA}$ become one of the most efficient enzymes in nature. Just owing to the extremely high catalytic efficiency, CA has displayed great potential in CO_2 capture and sequestration.

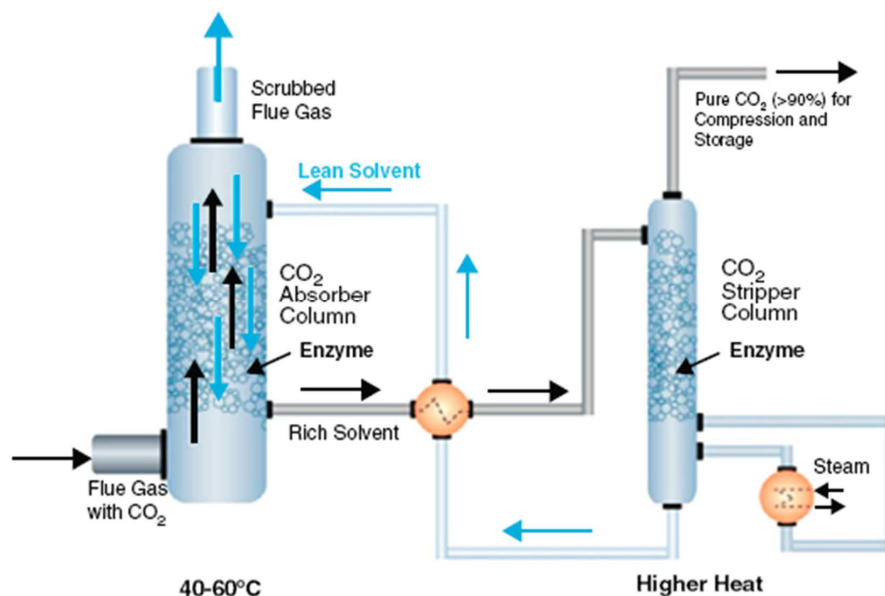


Figure 10. Schematic illustration of the combination of CA-catalytic CO₂ conversion process and chemical absorption process. Reproduced with permission from ref. 2. Copyright 2011 Elsevier.

To the best of our knowledge, the CA-catalytic conversion of CO₂ has been applied for assisting three techniques (absorption, membrane separation and precipitation/mineralization) during the CO₂ capture, sequestration & utilization.² One of the most successful cases should be the incorporation of CA-catalytic conversion of CO₂ into the chemical absorption of CO₂ with regenerable alkaline aqueous solvents. In traditional chemical absorption process, CO₂ was removed from the mixing gas (mainly refers to flue gas) in the absorber column and then desorbed in a heated stripper column to obtain relatively pure CO₂. In this process, the major challenge was as follows: the alkaline aqueous solvents bond CO₂ so tightly that the parasitic energy loss in desorbing CO₂ would double the cost of electricity. The combination of CA-catalytic conversion process and chemical absorption process would both increase the absorption rate of CO₂ in the alkaline aqueous solvents and facilitate the use of aqueous solvents with a lower heat/energy input for desorption (**Figure 10**). However, the relatively harsh conditions in the absorption processes (*i.e.* temperatures of 50-125 °C; high concentrations of organic amine; trace contaminants) may cause the denaturation of enzyme, and reduce the enzyme activity/stability. To overcome this limitation, several approaches have been developed, including sourcing CA from thermophilic organisms, creating thermo-resistant CA by protein engineering techniques, immobilizing CA in/on suitable supports, and modifying the absorption process. As a very recent example, Lu and coworkers²⁹ developed a potassium carbonate-based absorption process for absorbing CO₂ from coal combustion flue gas, where CA was used to accelerate the CO₂ absorption process. To enhance the enzyme

stability (including thermal/chemical resistance), CA was immobilized on nonporous silica-based nanoparticles. After conducting the absorption process in an alkaline solution over a 60-d period at 50 °C, the immobilized CA could retain 56-88% of its original activity, while only 30% of original activity was retained for the free CA. The second case should be membrane separation technique assisted by the CA-catalytic conversion process, which was first conducted by Trachtenberg's and Chen's groups.^{30,31} The constructed CA "permeator" was mainly composed of two hollow fiber microporous membranes (feed fiber membrane and sweep fiber membrane) separated by a CA-containing liquid medium. During the separation process, CO₂ in the feed gas was diffused to the external surface of the feed fiber membrane, contacted with CA in the liquid medium, and then efficiently hydrated into bicarbonate catalyzed by CA (**Figure S7**).³¹ The generated bicarbonate was subsequently diffused across the matrix of the liquid medium to the outer surface of the sweep fiber membrane, where dehydration of bicarbonate took place. The acquired CO₂ was finally released to the sweep fiber membrane. Collectively, the incorporation of CA in the membrane process can enhance the separation efficiency through increasing both the absorption and desorption rates of CO₂. This design may offer a mild and efficient alternative for converting and gathering CO₂ with high purity in comparison to the first case of alkaline scrubbing system. However, some serious drawbacks were appeared, such as the increased operation cost resulting from the requirement of the vacuum condition and the pre-treatment of the feed gas (for removing the membrane-damaged component, *e.g.*, SO_x and heavy metals). As a third case for converting CO₂ into bicarbonate catalyzed by CA, the precipitation/mineralization of the as-formed bicarbonate into water-insoluble CaCO₃ has also attracted numerous interests. This was primarily ascribed to the following two reasons: 1) CaCO₃ minerals were physically/chemically stable for thousands of years, averting the release of CO₂ back to the atmosphere naturally; 2) the mechanical strength and stability of CaCO₃ minerals made them well-suited as inputs for manufacturing processes or building-block materials. For instance, Jeong and co-workers³² firstly accelerated the CO₂ absorption rate by the sterically hindered amine 2-amino-2-methyl-1-propanol (AMP) in the presence of CA, and then converted the absorbed product into CaCO₃. The catalytic efficiency (k_{cat}/K_m) and CO₂ absorption capacities of AMP in the presence or absence of CA were 2.61×10^6 or $1.35 \times 10^2 \text{ M}^{-1} \text{ s}^{-1}$, and 0.97 or 0.96 mol mol⁻¹(AMP), respectively, suggesting a rather positive effect of CA in the CO₂ absorption process. Further carboxylation process was performed by using various Ca²⁺ sources, such as Ca(OOCCH₂CH₃)₂ (CAP), CaCl₂ (CAC) and Ca(OOCCH₃)₂ (CAA), to produce CaCO₃ with various polymorphs. Although the CA-catalytic hydration of CO₂ accelerated the mineralization

efficiency, the recycling of CA was difficult to put into use. Considerable efforts have been dedicated to address this problem. Gu and co-workers³³ reported an CA-assisted approach to synthesize crystalline CaCO₃ composites accompanied with *in situ* entrapment of CA. In their work³³, free CA was primarily utilized as the catalyst for assisting the precipitation/mineralization process, where CA could be *in situ* entrapped in the CaCO₃ composites. CA immobilized in the CaCO₃ composites could retain *ca.* 43% activity of its free form. Since CaCO₃ was pH/temperature sensitive, which may restrict the application of the immobilized CA in some specific areas, other immobilization carriers and protocols were also explored. For instance, Patwardhan and co-workers³⁴ presented a green approach for recyclable conversion of CO₂ to CaCO₃ catalyzed by CA-encapsulated (bio)inspired silica (**Figure S8**). The simple, mild and cost-effective (bio)silicification process for CA immobilization made this protocol easy to scale up for industrial applications. Moreover, the immobilized CA exhibited comparable catalytic activity to the free CA, which displayed little enzyme leaching with excellent recycling/storage/thermal stabilities (**Table S2**, the ratio of the removed CO₂ content to the initial content was 86% for the immobilized CA, and 90% for the free CA). Directly expressing CA onto microorganism cells was an alternative approach to immobilize CA for enhancing the CO₂ absorption rate and CaCO₃ mineralization efficiency. One of the typical examples was proposed by Belcher and co-workers.³⁵ They constructed an enzymatically catalyzed CO₂ mineralization process in bench scale, and modelled/evaluated at industrial scale by using standard chemical process scale-up protocols. Specifically, a yeast display system from an engineered organism (*Saccharomyces cerevisiae*) was constructed and utilized to screen three CA isoforms (*i.e.*, human CA II, bovine CA II (bCA2) and a CA isoform from *Streptococcus thermophiles*) and several mineralization peptides (*e.g.*, GPA, N66, *etc.*) for investigating their influence on the CO₂ hydration process, CaCO₃ mineralization and particle settling rate. Among the several established systems, the bCA2-GPA-yeast system exhibited much higher rate for all the three steps in bench-scale measurements. Furthermore, an industrial-scale modeling evaluation was also conducted to investigate the cost-effectiveness of this bCA2-GPA-yeast combined system. The modeling result predicted that a process conducted by this bCA2-GPA-yeast combined system was *ca.* 10% cost effective per tonne of captured CO₂ than a CA-free process. The cost-effectiveness made the process comparable or even favorable to CO₂ capture by alkaline absorption process. Herein, it should also be noted that, for all the three CA-assistant techniques, the rate limiting step is still the mass transfer of CO₂ from gas phase to water, although CA-catalyzed process can accelerate this process through increasing the conversion rate of dissolved CO₂ to bicarbonate followed by

further removal or mineralization.

3.2.2 Conversion of CO₂ to biodegradable chemicals by decarboxylases (other lyases)

Besides CA, several other types of lyases (decarboxylases) existed in cells have also been explored for catalyzing the carboxylation of raw materials with CO₂ *in vitro*. The main target of the carboxylation by decarboxylases is to make toxic raw compounds more hydrophilic, thus reducing their affinity toward lipophilic biological components (*e.g.*, membranes, proteins, *etc.*). Interestingly, the decarboxylases do not belong to the enzyme involved in the six major routes of the CO₂ metabolic process and generally regarded as an enzyme that catalyzes the decarboxylation processes in cells. Since these decarboxylases can also reversibly catalyze the carboxylation of substrate with CO₂, it has gained a lot of attention in the past years. As summarized by Faber and co-workers,¹ four kinds of enzymatic carboxylation reactions derived from catabolic routes have been developed *in vitro*, including 1) carboxylation of epoxides, 2) carboxylation of aromatics, 3) carboxylation of hetero-aromatics, and 4) carboxylation of aliphatics.

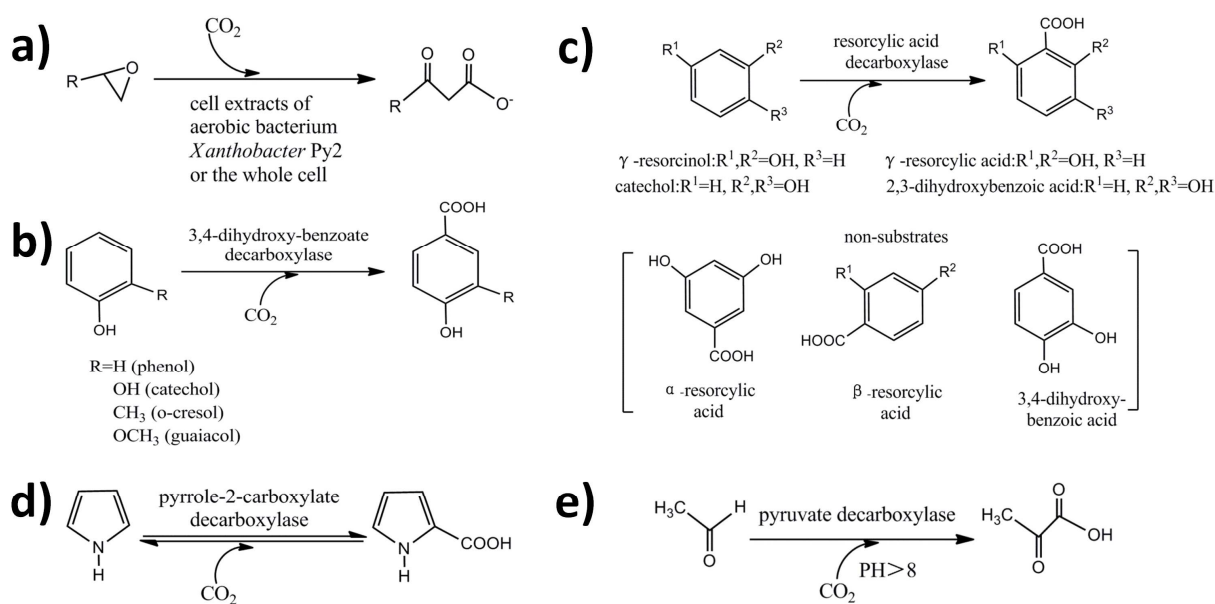


Figure 11. a) Biocatalytic carboxylation of epoxides by the cell extracts of aerobic bacterium *Xanthobacter* Py2 or the whole cell; b) regioselective *para*-carboxylation of non-activated phenolic compounds catalyzed by 3,4-dihydroxy-benzoate decarboxylase; c) regioselective (*ortho*) carboxylation of non-activated phenolic compounds catalyzed by resorcylic acid decarboxylases; d) carboxylation of pyrrole by pyrrole-2-carboxylate decarboxylase; and e) carboxylation of acetaldehyde by pyruvate decarboxylase.¹

For the first route of epoxides carboxylation, the exploration could be dated back to the 1990s (about 20

years ago). In these cases, cell extracts of *Xanthobacter* Py2 or the whole cell rather than purified enzymes were applied for the carboxylation of epoxides (**Figure 11a**), which restricted the further *in vitro* application of this route. For the second route of aromatics carboxylation, initially, the cell extracts or partially purified phenylphosphate enzymes of *Thauera aromatica* were applied for the carboxylation of phenol with CO₂ to synthesize *p*-hydroxybenzoic acid at ambient conditions. A turnover number of *ca.* 16000 with a high selectivity toward *p*-hydroxybenzoic acid (~100%) could be acquired. Further attempt of enhancing the enzyme stability was also conducted through immobilizing the enzymes on the low-melting agar.³⁶ Alternatively, purified 4-hydroxybenzoate decarboxylases from *Chlamydomophila pneumoniae* AR39, *Enterobacter cloacae* P240109 and *Clostridium hydroxybenzoicum* could also catalyze the reversible carboxylation of phenol with CO₂ to yield 4-hydroxybenzoate. Similar to phenol, catechol could also be reversibly carboxylated into 3,4-dihydroxybenzoate in the presence of bicarbonate catalyzed by 3,4-dihydroxy-benzoate decarboxylase from *Clostridium hydroxybenzoicum* (**Figure 11b**). Nevertheless, in all above cases, the equilibrium strongly favoured the decarboxylation (carboxylation efficiency no higher than 19%). Besides the *regioselective* carboxylation in *para*-position to the phenolic hydroxyl group, some γ -resorcylic acid decarboxylases (or 2,6-dihydroxybenzoate decarboxylases) from *Agrobacterium tumefaciens*, *Rhizobium radiobacter* and *Rhizobium sp* have also been used to catalyze the *regioselective ortho*-carboxylation of 1,3-dihydroxybenzene (or γ -resorcinol) with CO₂. This carboxylation process produced only 2,6-dihydroxybenzoic acid (or resorcylic acid) without containing *regio*-isomeric α - or β -resorcylic acid acquired from *meta*-, or *para*-carboxylation (**Figure 11c**). For the third route of hetero-aromatics carboxylation, pyrroles as another kind of electron-rich heteroaromatics was considered as suitable substrates for enzymatic carboxylation. The carboxylation of pyrrole with CO₂ can be catalyzed by pyrrole-2-carboxylate decarboxylase from *Bacillus megaterium* and *Serratia sp*, where an organic acid (such as acetate, propionate, butyrate or pimelate) was adopted as a "cofactor" (**Figure 11d**, the possible reaction mechanism catalyzed by pyrrole-2-carboxylate decarboxylase in the presence of organic acid is proposed as shown in **Figure S9**). For the fourth route of aliphatics carboxylation, pyruvate decarboxylase from *Brewer's yeast* was successfully applied for the carboxylation of acetaldehyde with CO₂ to synthesize pyruvate, where thiamine pyrophosphate (TPP) was utilized as a cofactor (**Figure 11e**).³⁷ To acquire high enzymatic activity, operational conditions especially the pH values were tailored to manipulate the carboxylation process. As a result, the highest pyruvate yield (81%) was obtained at pH 11 in aqueous sodium bicarbonate buffer that was served both as solvent and CO₂-source. In order to give a

clearer illustration about the extracted/purified enzymes that have been applied for carboxylation, **Table S3** was provided according to previous literature.¹

4. Conversion of CO₂ by multienzyme *in vitro*

To synthesize specific product from CO₂ *in vivo*, cells usually integrate several kinds of enzymes (including the enzyme that directly fixes/converts CO₂ and other enzymes that conduct the subsequent reactions) to implement multienzyme reactions. Additionally, the hierarchical structure and suitable microenvironment of cells ensure the efficient and ordered processing of a series of catalytic reactions. Enlightened by this, several multienzyme routes have been developed to produce target fuels/chemicals/materials. This section will describe the state-of-the-art routes to the catalytic conversion of CO₂ by multienzyme. Besides, the existing form of multienzyme in cells also offer efficient and promising ways to construct multienzyme systems *in vitro*, which will also be described in this section.

4.1 Conversion of CO₂ to methanol by multiple dehydrogenases

Converting CO₂ into methanol by multienzyme has been recognized as one of the most promising roadmaps due to the following two attributes: 1) the recycling of the "greenhouse" gas, and 2) the efficient production of sustainable/renewable fuel alternatives. In comparison to the fuels (CO, methane, *etc.*) from the single-enzyme route, the liquid methanol produced from the multienzyme reaction has much higher energy capacity and is easier to transport. For the first time, Yoneyama and co-workers³⁸ reported the successful electrochemical reduction of CO₂ to methanol with F_{ate}DH and methanol dehydrogenase (MDH) as the catalysts and pyrroloquinolinequinone (PQQ) as a cofactor. This approach afforded a facile route for the generation of methanol directly from CO₂ under mild conditions. As described in Yoneyama's report,³⁸ the type of the cofactors greatly influenced the reduction behavior of CO₂ and an appropriate cofactor can improve the rate of this multienzyme reaction. To take the advantage of the fact that dehydrogenases can effectively catalyze the reduction of CO₂ in the presence of a suitable cofactor, Dave and co-workers³⁹ reported a consecutive reduction approach of CO₂ to methanol with three dehydrogenases as the catalysts and NADH as a cofactor. The overall reaction process was shown in **Figure 12**.

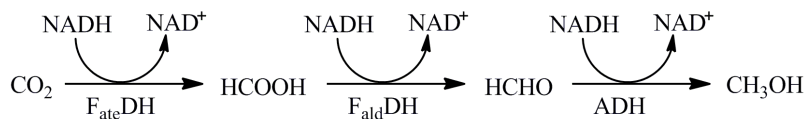


Figure 12. Reaction route of CO₂ to methanol catalyzed by three dehydrogenases (F_{ate}DH-formate dehydrogenase; F_{ald}DH-formaldehyde dehydrogenase; ADH-alcohol dehydrogenase).³⁹

As shown in **Figure 12**, CO₂ was reduced into formate by F_{ate}DH in the first step, followed by the reduction of formate to formaldehyde catalyzed by formaldehyde dehydrogenase (F_{ald}DH) in the second step. Methanol was produced from the reduction of formaldehyde by alcohol dehydrogenase (ADH) in the final step. In all the three steps, NADH acted as a cofactor for each dehydrogenase-catalyzed reduction step. The thermodynamic feasibility of this multienzyme reduction of CO₂ to methanol was investigated by Wang and co-workers.⁴⁰ They pointed out that this multienzyme reaction was highly sensitive to the pH value of the reaction medium. The reactions should be conducted under the conditions of lower pH values and ionic strength with elevated temperatures. However, such conditions usually induced the denaturation and inactivation of the native enzymes. The physicochemical stabilization approaches (*i.e.*, immobilization) should be then incorporated. For instance, Dave and co-workers³⁹ co-encapsulated the three dehydrogenases in a porous silica sol-gel matrix and found that the methanol yield/production was substantially increased compared to that from the free enzymes. They ascribed the enhanced methanol yield/production to the confinement of the multienzyme in the nanopores of silica gels that favourably altered the reaction thermodynamics and final equilibrium.

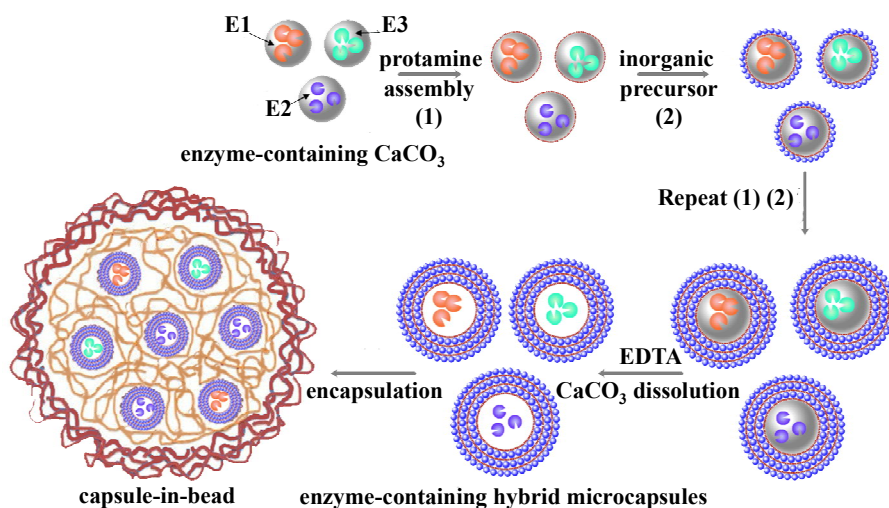


Figure 13. Schematic preparation process of multienzyme system based on a capsule-in-bead scaffold. (E1: F_{ate}DH, E2: F_{ald}DH, E3: ADH) Reproduced from ref. 43. Copyright 2009 Royal Society of Chemistry.

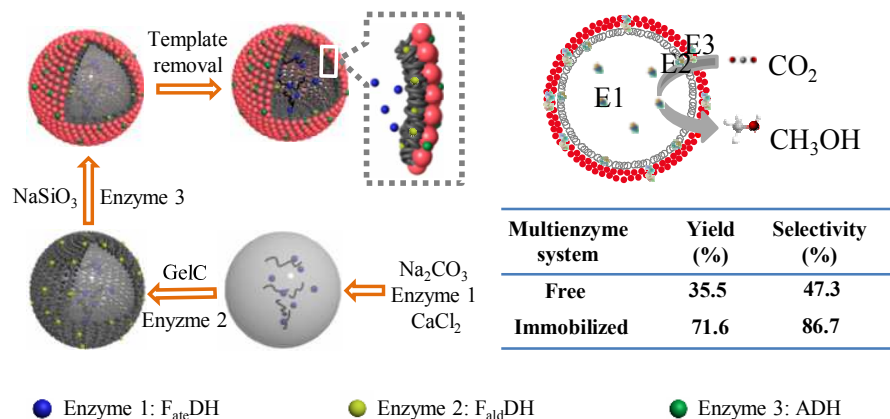


Figure 14. Schematic preparation process of multienzyme system based on an ultrathin, hybrid microcapsule; schematic illustration of the multienzyme reaction from CO₂ to methanol; and the yield and selectivity of the free enzymes and multienzyme system. (E1: F_{ate}DH, E2: F_{ald}DH, E3: ADH) Reproduced from ref. 44. Copyright 2014 American Chemical Society.

With the focus on screening suitable immobilization approaches, Jiang's group has carried out a series of investigations on the multienzyme conversion of CO₂ in recent years.⁴¹⁻⁴⁴ Different kinds of immobilization approaches and carriers have been designed to create nature-mimic microenvironments for enzymes. For example, the three dehydrogenases were co-encapsulated in the alginate-silica composites. The activity retention, storage stability/reusability of the enzymes were significantly enhanced compared to those of the free enzymes.⁴¹ This phenomenon could be owing to the more suitable microenvironment of the alginate-silica composites, including high hydrophilicity, moderate rigidity and flexibility, optimized cage confinement effect, and short diffusion distance. As a relatively novel concept, biomineralization process can open a promising avenue to enzyme immobilization under mild conditions. By mimicking the biomineralization process, the three dehydrogenases were co-immobilized in TiO₂ nanoparticles using protamine as an inducer under mild conditions. The three dehydrogenases could construct an enzymatic "assembly line" to convert CO₂ into methanol. Therefore, a high yield of methanol was obtained.⁴² However, co-immobilization of the three enzymes within one support usually suffered from the following limitations: 1) the activities of the enzymes may be influenced by the undesirable interaction among different enzymes; 2) it was difficult to manipulate the immobilization process or the catalytic behavior of the individual enzyme. To allow the sequential reactions occurred within a well-defined reaction zone, a capsules-in-bead scaffold for spatially separated multienzyme system was constructed.⁴³ As shown in **Figure 13**, the "guest" capsules were prepared through the combination of biomimetic mineralization and layer-by-layer (LbL) assembly by using enzyme-containing CaCO₃

microparticles as sacrificial templates. After that, the "guest" capsules were produced and then co-encapsulated into the larger "host" alginate beads to form the capsules-in-bead scaffold. The three dehydrogenases were located separately in this scaffold and used to convert CO₂ into methanol. Compared with the three dehydrogenases co-encapsulated in an alginate gel bead, the dehydrogenases encapsulated in the capsules-in-bead support showed higher initial activity and enhanced methanol yield. This may be ascribed to the reduced interference among different enzymes, elevated local concentration of the intermediate products, and shorter diffusion distance of the intermediate from the active site of an enzyme to another. To further realize the flexible regulation of individual enzyme and reduce the mass transfer resistance, an ultrathin, hybrid microcapsule for multienzyme system was constructed to convert CO₂ into methanol through the coupling of biomimetic mineralization and biomimetic adhesion (**Figure 14**).⁴⁴ Three dehydrogenases of F_{ate}DH, F_{ald}DH, and ADH, were immobilized in the capsule lumen, the organic layer of the capsule wall, and the silica layer of the capsule wall, respectively. The yield and selectivity of this multienzyme system (71.6% and 86.7%) were remarkably higher than those of the free multienzyme system (35.5% and 47.3%).

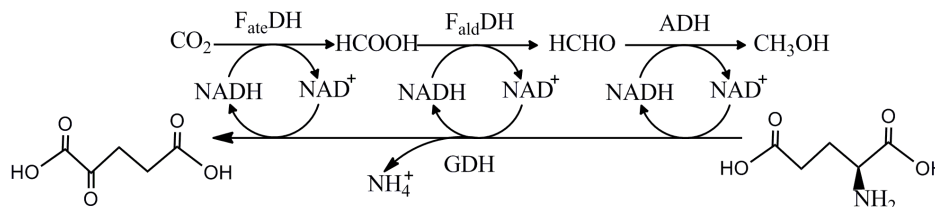


Figure 15. The multienzyme route for the synthesis of methanol from CO₂ by three dehydrogenases with *in situ* regeneration of NADH.⁴⁵ (GDH: glutamate dehydrogenase)

As shown in **Figure 12** and the investigations as described above, the synthesis of one mole of methanol would consume three moles of NADH. However, the high cost of NADH would hamper the further application of CO₂ conversion in large-scale operations. Suitable NADH regeneration/reuse strategies may provide a solution to address the above problem and became an important research issue. Wang and co-workers⁴⁵ investigated the feasibility of methanol production from CO₂ with an *in situ* cofactor regeneration system. (**Figure 15**) Four enzymes including F_{ate}DH, F_{ald}DH, ADH and glutamate dehydrogenase (GDH) were co-immobilized on the same particle, while NADH was immobilized on the other particle. GDH was used for the *in situ* regeneration of NADH driven by the dehydrogenation of glutamate to 2-oxoglutarate. Although the productivity of methanol was lower than that of the free multienzyme system, the immobilized multienzyme system showed fairly good recycling stability. After recycling for 7 times, more than 80% of its original

productivity can be maintained and the cumulative methanol yield calculated based on the amount of the cofactor can reach 127%. Compared to the single-batch yield of 12% in the free multienzyme system, a significant enhancement in cofactor utilization was obtained by using this immobilized multienzyme system. Next, Galarneau and co-workers⁴⁶ incorporated another regeneration system to increase the activity of the multienzyme system. They compared three different NADH regeneration systems and found that phosphate dehydrogenase (PTDH) worked most efficiently. The four dehydrogenases ($F_{\text{ate}}\text{DH}$, $F_{\text{ald}}\text{DH}$, ADH, PTDH) were then co-encapsulated in phospholipids-silica nanocapsules with the internal diameter of *ca.* 30 nm. After assessment of the catalytic performance of the immobilized multienzyme system, an activity of 55 times higher than that of the free multienzyme system can be obtained. All these reports indicated that the incorporation a NADH regeneration system was a useful way to improve the catalytic activity and stability of the multienzyme.

4.2 Conversion of CO_2 to other fuels/chemicals/materials by multienzyme

Although the conversion of CO_2 to methanol through multiple dehydrogenases offers us a promising route for simultaneously consuming CO_2 (*greenhouse gas*) and acquiring methanol (*fuel/chemical*), developing novel reaction routes for directly producing advanced fuels/chemicals/materials with higher numbered carbon ($>\text{C}1$) would be also highly competitive.

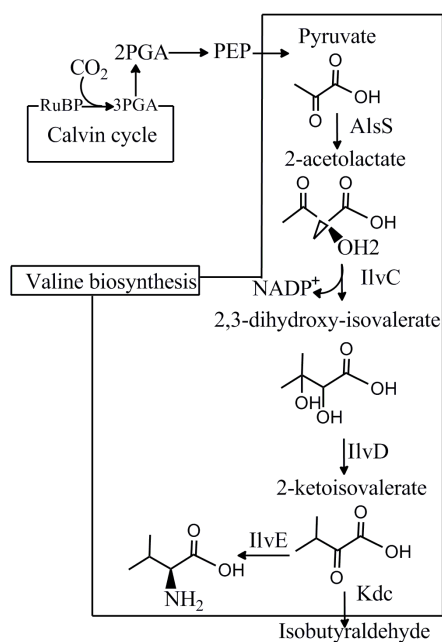


Figure 16. The multienzyme route for the synthesis of isobutyraldehyde from CO_2 . AlsS: acetolactate synthase; IlvC: acetohydroxy acid isomeroreductase; IlvD: dihydroxy-acid dehydratase; Kdc: 2-ketoacid decarboxylase.⁴⁷

One encouraging advance was the photosynthetic recycling of CO_2 into isobutyraldehyde, which was

conducted by Liao and co-workers (**Figure 16**).⁴⁷ They genetically engineered *Synechococcus elongatus* PCC7942 through the expression of several key genes (*alsS*, *ilvC* and *ilvD*) to produce isobutyraldehyde from CO₂. The primary steps for the CO₂ conversion process can be found in **Figure 16**, where Rubisco, acetolactate synthase (AlsS), acetohydroxy acid isomeroreductase (IlvC), dihydroxy-acid dehydratase (IlvD) and 2-ketoacid decarboxylase (Kdc) were the five key enzymes. Since Rubisco was the bottleneck in carbon fixation in *Cyanobacteria*, overexpression of this enzyme could increase the reaction rate of CO₂. Accordingly, the productivity of isobutyraldehyde could be increased. In Liao's work,⁴⁷ although several single-enzyme routes were combined for converting CO₂ into target molecules, the multienzyme reaction was actually occurred *in vivo* (*Cyanobacteria*) rather than *in vitro*. Inspired by this *in vivo* engineered CO₂ conversion process, Wendell and co-workers⁴⁸ constructed an *in vitro* artificial photosynthesis system through engineering the essential enzymes in the Calvin cycle and an ATP-producing photoconversion system (also denoted as BR/F₀F₁-ATP vesicles) into foam architectures (**Figure S10**). During this process, the Tungara frog surfactant protein (Ranaspumin-2) was required to allow the coupled enzymes and BR/F₀F₁-ATP vesicles to be concentrated into the Plateau channels of the foam. The artificial photosynthesis system could be successfully utilized for converting CO₂ into sugars (*e.g.*, glucose) with a conversion ratio of *ca.* 96%. According to the report,⁴⁸ the glucose-producing capability of this photosynthesis system was 116 nmol (glucose) mL⁻¹ h⁻¹. It was also assumed that if a foam architecture containing the glucose-producing system was layered to 1 m in height and the conversion ratio of sugar to 2,5-dimethylfuran was 88%, this artificial photosynthesis system could have the capability to produce 10 kg ha⁻¹ of 2,5-dimethylfuran per hour. Furthermore, suppose that a hectare of foam could receive sunlight of 11 h day⁻¹, a productivity of 34.5 t ha⁻¹ a⁻¹ of 2,5-dimethylfuran could be achieved, which was 10 times higher than that of DMF (3.4 t ha⁻¹ a⁻¹) from biomass.

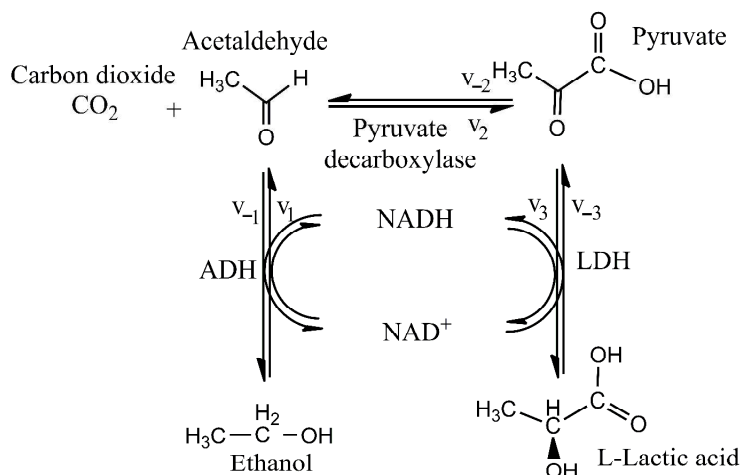


Figure 17. The multienzyme route for the synthesis of L-Lactic acid from CO₂ and ethanol.⁴⁹

Recently, Wang and co-workers⁴⁹ explored a relatively simpler multienzyme route for converting CO₂ and ethanol into L-Lactic acid, which donated a novel and sustainable alternative way to synthesize building blocks for biodegradable polymers. As shown in **Figure 17**, the catalytic process mainly consisted of three single-enzyme routes: 1) the oxidation of ethanol to acetaldehyde by ADH in the presence of NAD⁺, 2) the synthesis of pyruvate from CO₂ and acetaldehyde catalyzed by pyruvate decarboxylase, and 3) the reduction of pyruvate to L-Lactic acid by lactate dehydrogenase (LDH) in the presence of NADH. Obviously, the cycling of NAD⁺/NADH could be achieved *via* the first and third single-enzyme route. Another interesting result in their research was that the reaction kinetics for each individual reaction remained unaltered in the multienzyme reaction. Therefore, the kinetic parameters determined from individual reaction could be directly employed for the prediction of the mixed reaction kinetics.

5. Future perspectives

Enzymatic conversion for CO₂ capture, sequestration & utilization provides us a green and promising approach to reduce the global warming and climate changes. Inspired by the CO₂ metabolic process in cells, two classes of enzymes (oxidoreductases and lyases) have been successfully utilized for converting CO₂ into different kinds of fuels/chemicals/materials. To enhance the efficiency of the enzyme catalytic process, various technologies or approaches have been reported for rational preparation of enzyme-based catalysts, optimization of reaction processes, and elucidation of reaction mechanisms.

Despite a large number of investigations, significant scientific and technical advances are still required for the large-scale utilization of the enzymatic conversion of CO₂. To our knowledge, the following aspects should be paid more attention on the future research. 1) The enzymes are generally expensive and sensitive catalysts which hinder their industrial applications, several approaches in bench scale (including enzyme modification, enzyme immobilization, *etc.*) have been developed to reduce the cost and improve the activity/stability of the enzymes. Screening some of these developed approaches and scaling up to industrial level are particularly desired. Furthermore, the recently explored methodology (*i.e.*, *de novo* computational enzyme design) can be implanted to create novel enzymes with specific properties for efficient CO₂ conversion, which offers an alternative opportunity for industrial application. 2) In the enzymatic conversion of CO₂, the cofactor-dependent reactions are widely involved. However, the high price and difficult availability of the ion-type cofactor (NADH, NADPH, *etc.*) severely restrict the large-scale applications. In this *tutorial review*,

we have introduced some representative approaches to regenerate and reuse the cofactors. These existing approaches usually consist of complicated reaction processes or expensive additives (such as noble metal-based mediator). Quite recently, converting CO₂ into formate by utilizing H₂ as low-cost and molecule-type "cofactor" was ingeniously proposed by Müller and co-workers. Thus, much more research efforts will be stimulated in discovering low-cost and low-energy-input approaches for the regeneration and reuse of the cofactor, or digging out novel enzymatic routes for the conversion of CO₂ with low-cost and easy-available "cofactors", or even exploring cofactor-independent enzymes, such as molybdenum- or tungsten- containing F_{atc}DH. 3) Many single-enzyme routes derived from metabolic process of CO₂ in cells pave the way for CO₂ capture, sequestration & utilization. However, only limited multienzyme routes (CO₂ to methanol, CO₂ to glucose, CO₂ to L-Lactic acid, *etc.*) have been constructed *in vitro*. It is therefore imperative to design a number of enzymatic routes and/or construct novel multienzyme systems for achieving the sustainable production of fuels/chemicals/materials from CO₂. 4) Utilization of CO₂ based on chemical, photochemical and electrochemical technologies has great application potentials. Thus, it is expected that integrating these routes with enzymatic route may increase the selectivity and productivity. For example, the combination of photo-/electro-catalysis with enzymes for the reduction of CO₂ to formate or CO has been reported by several research groups, including Hirst's and Armstrong's groups. These reports raise interesting and important issues associated with the integrations of biocatalysis with other technologies for efficient conversion of CO₂. In short, besides the chemical, photochemical and electrochemical conversion, enzymatic conversion of CO₂ has become a viable and promising approach for CO₂ capture, sequestration & utilization. Although it has been explored for many years, much more effort should be devoted to excavate facile and low-energy routes for CO₂ conversion by the cost-effective enzyme-based technologies.

Acknowledgements

The authors thank the financial support from the National Science Fund for Distinguished Young Scholars (21125627), National Natural Science Funds of China (21406163), and the Program of Introducing Talents of Discipline to Universities (B06006).

References

- 1 S. M. Glueck, S. Gümüş, W. M. Fabian and K. Faber, *Chem. Soc. Rev.*, 2010, **39**, 313-328.
- 2 C. K. Savile and J. J. Lalonde, *Curr. Opin. Biotechnol.*, 2011, **22**, 818-823.
- 3 M. Aresta, A. Dibenedetto and A. Angelini, *Chem. Rev.*, 2013, **114**, 1709-1742.
- 4 W. Wang, S. Wang, X. Ma and J. Gong, *Chem. Soc. Rev.*, 2011, **40**, 3703-3727.

- 5 E. V. Kondratenko, G. Mul, J. Baltrusaitis, G. O. Larrazabal and J. Perez-Ramirez, *Energy Environ. Sci.*, 2013, **6**, 3112-3135.
- 6 A. M. Appel, J. E. Bercaw, A. B. Bocarsly, H. Dobbek, D. L. DuBois, M. Dupuis, J. G. Ferry, E. Fujita, R. Hille, P. J. A. Kenis, C. A. Kerfeld, R. H. Morris, C. H. F. Peden, A. R. Portis, S. W. Ragsdale, T. B. Rauchfuss, J. N. H. Reek, L. C. Seefeldt, R. K. Thauer and G. L. Waldrop, *Chem. Rev.*, 2013, **113**, 6621-6658.
- 7 G. Fuchs, *Annu. Rev. Microbiol.*, 2011, **65**, 631-658.
- 8 R. K. Thauer, *Science*, 2007, **318**, 1732-1733.
- 9 R. Castillo, M. Oliva, S. Martí and V. Moliner, *J. Phys. Chem. B*, 2008, **112**, 10012-10022.
- 10 M. Beller and U. T. Bornscheuer, *Angew. Chem. Int. Ed.*, 2014, **53**, 4527-4528.
- 11 Y. Amao, N. Shuto, K. Furuno, A. Obata, Y. Fuchino, K. Uemura, T. Kajino, T. Sekito, S. Iwai, Y. Miyamoto and M. Matsuda, *Faraday Discuss*, 2012, **155**, 289-296.
- 12 R. K. Yadav, J. O. Baeg, G. H. Oh, N. J. Park, K. J. Kong, J. Kim, D. W. Hwang and S. K. Biswas, *J. Am. Chem. Soc.*, 2012, **134**, 11455-11461.
- 13 T. Reda, C. M. Plugge, N. J. Abram and J. Hirst, *Proc. Natl. Acad. Sci. USA*, 2008, **105**, 10654-10658.
- 14 K. Schuchmann and V. Muller, *Science*, 2013, **342**, 1382-1385.
- 15 Y. Lu, Z. Y. Jiang, S. W. Xu and H. Wu, *Catal. Today*, 2006, **115**, 263-268.
- 16 H. Dobbek, *Coordin. Chem. Rev.* 2011, **255**, 1104-1116.
- 17 A. Bassegoda, C. Madden, D. W. Wakerley, E. Reisner and Judy Hirst, *J. Am. Chem. Soc.*, 2014, **136**, 15473-15476.
- 18 J. H. Jeoung and H. Dobbek, *Science*, 2007, **318**, 1461-1464.
- 19 W. Shin, S. H. Lee, J. W. Shin, S. P. Lee and Y. Kim, *J. Am. Chem. Soc.*, 2003, **125**, 14688-14689.
- 20 A. Parkin, J. Seravalli, K. A. Vincent, S. W. Ragsdale and F. A. Armstrong, *J. Am. Chem. Soc.*, 2007, **129**, 10328-10329.
- 21 T. W. Woolerton, S. Sheard, E. Reisner, E. Pierce, S. W. Ragsdale and F. A. Armstrong, *J. Am. Chem. Soc.*, 2010, **132**, 2132-2133.
- 22 T. W. Woolerton, S. Sheard, E. Pierce, S. W. Ragsdale and F. A. Armstrong, *Energy. Environ. Sci.*, 2011, **4**, 2393-2399.
- 23 Y. S. Chaudhary, T. W. Woolerton, C. S. Allen, J. H. Warner, E. Pierce, S. W. Ragsdale and F. A. Armstrong, *Chem. Commun.*, 2012, **48**, 58-60.
- 24 A. Bachmeier, V. C. C. Wang, T. W. Woolerton, S. Bell, J. C. Fontecilla-Camps, M. Can, S. W. Ragsdale, Y. S. Chaudhary and F. A. Armstrong, *J. Am. Chem. Soc.*, 2013, **135**, 15026-15032.

- 25 H. A. Hansen, J. B. Varley, A. A. Peterson and J. K. Norskov, *J. Phys. Chem. Lett.*, 2013, **4**, 388-392.
- 26 L. C. Seefeldt, M. E. Rasche and S. A. Ensign, *Biochemistry*, 1995, **34**, 5382-5389.
- 27 Z. Y. Yang, V. R. Moure, D. R. Dean and L. C. Seefeldt, *Proc. Natl. Acad. Sci. USA*, 2012, **109**, 19644-19648.
- 28 K. M. Merz and L. Banci, *J. Am. Chem. Soc.*, 1997, **119**, 863-871.
- 29 S. H. Zhang, H. Lu and Y. Q. Lu, *Environ. Sci. Technol.*, 2013, **47**, 13882-13888.
- 30 M. Trachtenberg, US Patent US20080003662, 2008.
- 31 Y. T. Zhang, L. Zhang, H. L. Chen and H. M. Zhang, *Chem. Eng. Sci.*, 2010, **65**, 3199-3207.
- 32 M. Vinoba, M. Bhagiyalakshmi, A. N. Grace, D. H. Chu, S. C. Nam, Y. Yoon, S. H. Yoon and S. K. Jeong, *Langmuir*, 2013, **29**, 15655-15663.
- 33 E. T. Hwang, H. Gang, J. Chung and M. B. Gu, *Green Chem.*, 2012, **14**, 2216-2220.
- 34 C. Forsyth, T. W. S. Yip and S. V. Patwardhan, *Chem. Commun.*, 2013, **49**, 3191-3193.
- 35 R. Barbero, L. Carnelli, A. Simon, A. Kao, A. D. Monforte, M. Ricco, D. Bianchi and A. Belcher, *Energy Environ. Sci.*, 2013, **6**, 660-674.
- 36 M. Aresta and A. Dibenedetto, *Rev. Mol. Biotechnol.*, 2002, **90**, 113-128.
- 37 M. Miyazaki, M. Shibue, K. Ogino, H. Nakamura and H. Maeda, *Chem. Commun.*, 2001, 1800-1801.
- 38 S. Kuwabata, R. Tsuda and H. Yoneyama, *J. Am. Chem. Soc.*, 1994, **116**, 5437-5443.
- 39 R. Obert and B. C. Dave, *J. Am. Chem. Soc.*, 1999, **121**, 12192-12193.
- 40 F. S. Baskaya, X. Y. Zhao, M. C. Flickinger and P. Wang, *Appl. Biochem. Biotechnol.*, 2010, **162**, 391-398.
- 41 S. W. Xu, Y. Lu, J. Li, Z. Y. Jiang and H. Wu, *Ind. Eng. Chem. Res.*, 2006, **45**, 4567-4573.
- 42 Q. Y. Sun, Y. J. Jiang, Z. Y. Jiang, L. Zhang, X. H. Sun and J. Li, *Ind. Eng. Chem. Res.*, 2009, **48**, 4210-4215.
- 43 Y. J. Jiang, Q. Y. Sun, L. Zhang and Z. Y. Jiang, *J. Mater. Chem.*, 2009, **19**, 9068-9074.
- 44 X. L. Wang, Z. Li, J. F. Shi, H. Wu, Z. Y. Jiang, W. Y. Zhang, X. K. Song and Q. H. Ai, *ACS Catal.*, 2014, **4**, 962-972.
- 45 B. El-Zahab, D. Donnelly and P. Wang, *Biotechnol. Bioeng.*, 2008, **99**, 508-514.
- 46 R. Cazelles, J. Drone, F. Fajula, O. Ersen, S. Moldovan and A. Galarneau, *New J. Chem.*, 2013, **37**, 3721-3730.
- 47 S. Atsumi, W. Higashide and J. C. Liao, *Nat. Biotechnol.*, 2009, **27**, 1177-1182.
- 48 D. Wendell, J. Todd and C. Montemagno, *Nano Lett.*, 2010, **10**, 3231-3236.
- 49 X. D. Tong, B. El-Zahab, X. Y. Zhao, Y. Y. Liu and P. Wang, *Biotechnol. Bioeng.*, 2011, **108**, 465-469.